Photocopying Living Chains. 2. Time-Dependent Measurements

Erdem Karatekin,[†,‡] Margaret Landis,[§] George Lem,[∥] Ben O'Shaughnessy,[*,⊥] and Nicholas J. Turro[‡]

Department of Chemistry, Columbia University, New York, New York 10027; Central Research Division, Pfizer Inc., Eastern Point Road, Groton, Connecticut 06340; Firmenich Chemical Manufacturing Center, 150 Firmenich Way, Port Newark, New Jersey 07114; and Department of Chemical Engineering, Columbia University, New York, New York 10027

Received January 16, 2001; Revised Manuscript Received July 20, 2001

ABSTRACT: In the preceding article, we reported a novel experimental technique, the "photocopy" method, that allowed the first ever measurements of living chain molecular weight distributions (MWDs) in free radical polymerization (FRP) at steady state. The method entails flooding the FRP at some instant with "photoinhibitor" radicals created photochemically from an appropriate precursor using a short laser pulse. These radicals are extremely slow in initiating new living chains, yet they couple with existing ones (and one another) at near diffusion-controlled rates and carry a fluorescent label. The effect is to freeze the growth of and simultaneously label the living chains that existed just before the laser pulse. In this article we first address the issue of photoinhibitor radical addition to monomer (at rate τ_{add}^{-1}), which creates new unwanted labeled living chains that distort the labeled living MWD measurements. Being unable to measure τ_{add}^{-1} by standard methods due to its extremely small value, we have studied the dependence of the total detected amount of labeled chains on the concentration of photoinhibitor radicals produced per pulse. These experiments suggest, albeit indirectly, that pollution should have a small effect when the photoinhibitor molecule di(1-naphthyl, phenyl methyl) sulfone (DNPMS) is used. Second, we present measurements of living chains whose steady state is perturbed by a series of photocopying pulses, applied with a period shorter than the time required to reestablish the steady state. These pulses have a dual role: (i) with each pulse all living chains are removed from the FRP instantly, creating a "vacuum" at $t = 0$, and (ii) the MWD of the living chains recovering toward steady state is "copied" into a labeled dead MWD. In this "reverse post-effect" experiment, monitoring the concentration $\psi_l(t)$ and the mean length $\bar{N}(t)$ of living chains as a function of laser period t_o, allows us to estimate the propagation velocity v_p (number of monomers added to a living chain per second) and the mean steady-state living chain lifetime τ^o_{living}.

I. Introduction

In the preceding article,[1] we presented a novel "photocopy method" which, for the first time, allowed the measurement of living chain molecular weight distributions (MWDs) in free radical polymerizations (FRPs). We saw that the measurement of this fundamental quantity during steady state FRPs provided the first direct test of predictions made on the living MWDs more than half a century ago.[2] It was found that chains longer than a certain length indeed follow an exponential distribution, in accord with the classical predictions of Flory and Schulz.[2] However, for shorter chains we found important deviations from the Flory−Schulz theory, consistent with predictions of recent FRP theories[3−6] incorporating the chain length dependence of the termination rate constants for reactions between propagating radicals, i.e., "living chains". It was also directly confirmed for the first time that the dead MWD is considerably sharper than the living one, as a fraction of the living chains terminate via coupling, as predicted by Schulz[2] in 1939. Using the measured MWDs of living chains at steady state, living chain concentrations ψ_l^o, mean living chain lengths $\bar{N}_o$, mean dead chain lengths $\bar{N}_d$, and f_d, the fraction of living chains terminating via disproportionation, were obtained directly. Coupling these direct measurements with reliable propagation velocities $v_p \equiv k_p[mon]$ (number of monomers added per second to a growing chain; k_p = propagation rate constant and [mon] = monomer concentration), reported in the literature, mean living chain lifetimes, $\tau^o_{living} \equiv \bar{N}_o/v_p$, termination rate constants, $k_t = 1/(\tau^o_{living}\,\psi_l^o)$, and rates of polymerization, $R_p = v_p\psi_l^o$, were obtained. We are aware of no other experimental method in the field of FRP capable of providing so many FRP parameters at once.[7,8] The FRP parameters obtained using the photocopy method were, overall, consistent internally and with independent estimates and values reported in the literature.

Nevertheless, we could not exclude the possibility of some side reactions affecting our results, at least for the measurements of short chain distributions. One of these side reactions is the addition of the special "photoinhibitor" radicals carrying a label, used in the novel photocopy method, to monomer, creating new, unintentionally labeled living chains, or "pollutants", (Figure 1) which would be measured along with the intentionally labeled ones (Figure 2). Such a side reaction would also explain the somewhat high values measured for the living chain concentrations (and hence polymerization rates) using the photocopy method. Thus, the first part of this article is concerned with the issue of photoinhibitor radical addition to monomer. We establish,

* To whom correspondence should be addressed: E-mail: bo8@columbia.edu.

† Present address: Institut Curie, Section de Recherche, Laboratoire PCC, UMR 168, 11, rue Pierre et Marie Curie, 75231 Paris Cedex 05, France.

‡ Department of Chemistry, Columbia University.

§ Pfizer Inc.

∥ Firmenich Chemical Manufacturing Center.

⊥ Department of Chemical Engineering, Columbia University.

10.1021/ma0100798 CCC: $20.00
Published on Web 10/12/2001

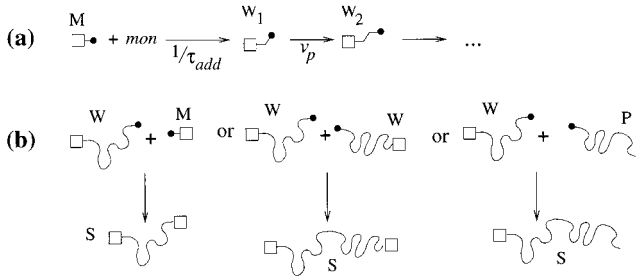

Figure 1. (a) When photoinhibitor radicals (M) add to monomer (at rate $1/\tau_{add} \ll v_p$) labeled chains W are produced, which grow at rate v_p. (b) Possible termination modes for W. All modes result in either singly or doubly labeled dead chains S.

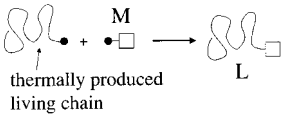

Figure 2. When photoinhibitor radicals (M) couple with thermally produced living chains, correctly labeled dead chains (L) are produced.

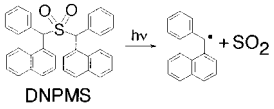

Figure 3. Photolysis of the photoinhibitor di(1-naphthyl, phenyl methyl) sulfone (DNPMS) producing 1-benzylnaphthyl radicals, which add very slowly to monomer, yet couple with living chains (and one another) at near diffusion-controlled rates.

using simple arguments, the conditions under which addition is expected to have an important effect on the measured living MWDs. We then present experiments testing the importance of photoinhibitor addition to monomer, suggesting that addition appears to be sufficiently slow for the photoinhibitor di(1-naphthyl, phenyl methyl) sulfone (DNPMS), shown in Figure 3, used to obtain the results presented in the preceding article.[1]

Another unwanted reaction is due to the fact that initiation of new living chains through thermal decomposition of the initiator persists during the photocopying process.[1] Thus, some post-laser-pulse initiated living chains will react with surviving photoinhibitor radicals, creating labeled dead chains which distort the measured MWD from that of the steady state living chains. This effect will be considered in detail in a future publication.[9] We note that this type of distortion can be completely eliminated by using photoinitiation instead of thermal initiation as discussed in section IV.

The second part of the present article concerns preliminary experiments in which poly(methyl methacrylate) (PMMA) living chains are perturbed from their steady state. Measuring MWDs of these chains is in fact much more informative than measuring simply steady-state distributions which was the subject of the preceding article.[1] The non-steady-state experiments allow living chain lifetimes, τ^o_{living}, and propagation velocities, v_p, to be *directly* measured using the photocopy method, completing the full array of parameters that can be measured in FRP (chain transfer constants, which are not measured here can also, in principle, be measured using the photocopy method, as discussed in section III.B).

The photocopy method is based on the following idea. The initial FRP mixture contains small amounts of thermal initiator (azobis(isobutyronitrile)—AIBN) dissolved in neat monomer (methyl methacrylate—MMA) as in conventional bulk FRP. However, in addition to initiator, a small amount of "photoinhibitor" molecules, such as DNPMS, shown in Figure 3, are also present. As the argon-saturated samples are placed in a thermostat at 60 °C, the initiator AIBN starts decomposing, producing highly reactive radicals which attack the surrounding monomer. These addition events result in the attachment of a monomer molecule to the original radical, and the transfer of the active radical site to the newly attached monomer. These one-step-propagated radicals in turn attack a new monomer, and a similar sequence of events follows. Propagation continues until the growth of a propagating radical ("living chain") is stopped through bimolecular reaction with another living chain. Soon after the polymerization starts, termination events provide a termination rate which balances the rate at which fresh living chains are initiated: a steady state is established. The photoinhibitor molecules do not interfere with the polymerization at these stages of thermal FRP, which last 2−5 min, and during which time conversion ϕ (fraction of monomer initially present converted to polymer) remains low ($\lesssim$1%). However, at some point during the polymerization, a very short laser pulse at the appropriate wavelength is applied which efficiently and selectively photolyzes the photoinhibitor molecules to produce photoinhibitor radicals. These radicals ideally possess the following very special properties: (i) they are extremely slow in adding to monomer, that is in initiating new living chains, (ii) they couple with one another and existing living chains at near diffusion-controlled rates, and (iii) they carry a fluorescent label. Thanks to these properties, when the FRP system is flooded by photoinhibitor radicals (when the number of photoinhibitor radicals produced by the laser pulse greatly exceeds the number of living chains present in the system) nearly all living chains are killed by photoinhibitor radicals during a time scale that is short compared to the mean living chain lifetime. The effect is to freeze the growth of living chains and to label them simultaneously. Thereafter, these labeled dead chains which, provided the photoinhibitors behave ideally, represent a good copy of the living chains that existed just before the laser pulse, are detected selectively thanks to the label they carry when their MWD is analyzed using gel permeation chromatography (GPC) equipped with a fluorescence (FL) detector. A refractive index (RI) detector in series with the FL detector gives information on unlabeled dead chains. Actually, 5−10 laser shots are used to accumulate labeled dead copies of living chains in order to improve signals. Further details on the experimental setup and the synthesis of photoinhibitors are given in the preceding article[1] and ref 10.

Before proceeding further, let us make a remark on our notation. We distinguish steady-state values from the corresponding non-steady-state ones by use of a sub- or superscript zero. Thus, mean living chain lengths are labeled $\bar{N}_o$, mean living chain lifetimes τ^o_{living}, and total living chain concentrations ψ^o_1 for their steady-state values. Further, roman scripts (L, P, M, etc.) refer to species, while italics (*L*, *P*, *M*, etc.) refer to concentrations of these species.

II. Photoinhibitor Radical Addition to Monomer

A. Addition Time, τ_{add}. When a FRP at low conversion is flooded with photoinhibitor radicals, the overwhelming majority of the living chains are killed by photoinhibitor radicals in a characteristic time scale $\tau_{kill} \equiv 1/k_{MP}M_o$, where M_o is the photoinhibitor radical concentration immediately following a laser flash, and k_{MP} is the photoinhibitor radical (M)—living chain (P) coupling rate constant. For sufficiently high M_o (for small values of the "flooding parameter" $r \equiv \psi_l^o/M_o$), τ_{kill} is much shorter than the mean living chain lifetime at steady state, $\tau^o_{living} \equiv 1/(k_t\psi_l^o)$, where k_t is the living chain termination rate constant and ψ_l^o is the steady state living chain concentration. The products of the living chain-photoinhibitor radical coupling reactions are labeled dead chains L (Figure 2). Effects due to propagation during the photocopying process introduce small errors to the measured living MWD of order $\tau_{kill}/\tau^o_{living}$, as discussed in refs 9 and 10. That is, if the photoinhibitors behave ideally (if they do not add to monomer), the distribution of labeled dead chains L is a good copy of the living chain distribution $\psi(N)$, provided the system is flooded with photoinhibitor radicals. Errors introduced by thermal initiation persisting during photocopying will be discussed in detail in a future publication.[9] At the end of this article, we present a photoinitiated version of the photocopy method wherein this unwanted effect is completely eliminated.

In practice, the addition rate of photoinhibitor radicals to monomer, $1/\tau_{add} \equiv k_{add}$[mon], where k_{add} is the rate constant for addition and [mon] is the monomer concentration, will be finite and some addition will occur (Figure 1). In this section, using simple arguments, we determine how large τ_{add} should be such that photoinhibitor addition to monomer will have a negligible effect on the measurement of the living population. We will see that the photocopy experiment is actually quite susceptible to addition of photoinhibitor radicals to monomer. This is because the FRP system is *flooded* with photoinhibitor radicals just following a laser pulse ($M_o \gg \psi_l^o$), and therefore even if a small fraction of the initial photoinhibitor radicals (M_o) adds to monomer, this may be a large amount compared to the tiny steady-state concentration of living chains (ψ_l^o) that the experiment attempts to measure.

Now, each photoinhibitor radical (M) addition to monomer (at rate $1/\tau_{add}$) produces a labeled 1-mer (W_1), which thereafter continues to grow at the usual propagation velocity v_p, as shown in Figure 1. These labeled growing chains, W (of any length), eventually produce incorrectly labeled dead chains (S) which cannot be distinguished experimentally from the labeled dead copy of the living chains (L) (of course, we can distinguish them conceptually in our theoretical model here). We note that *all* of the W species eventually produce labeled dead S species.

For the sake of simplicity, here we ignore initiation of fresh living chains through decomposition of thermal initiator. Furthermore, we will be concerned solely with the total amount, S_∞, of the S species produced due to addition of photoinhibitor radicals (M) to monomer. The effect of the pollution process on MWDs is considered in detail in ref 9. We will also assume the flooding parameter is small ($r \equiv \psi_l^o/M_o \ll 1$), so that nearly all living chains will be killed, and $L_\infty \equiv L(t \to \infty) \approx \psi_l^o$.

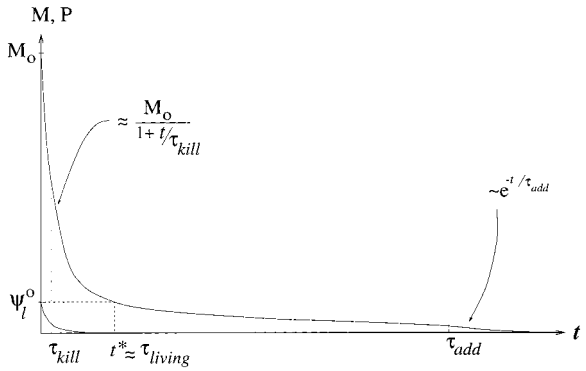

Figure 4. Schematic plot of the kinetics of M−P reactions (M = photoinhibitor radical, P = living chain), in the absence of thermal initiation, and when the reactivity of M toward addition to monomer is finite. By time $\tau_{kill} \equiv 1/(k_{MP}M_o)$, the concentration of M drops an amount of order 1 relative to its initial value, M_o. However, it takes a time $t^* \gg \tau_{kill}$ for M to become comparable to ψ_l^o, the steady state concentration of living chains that are to be measured. Addition of M to unpolymerized monomer will produce labeled chains (Figure 1) of an amount small compared to ψ_l^o, only if $\tau_{add} \gg t^*$, where τ_{add} is the first-order addition time scale. It is shown (see text) that $t^* \approx \tau^o_{living}$.

Clearly, if the total amount of incorrectly labeled dead chains, S_∞, is much less than the total amount of correctly labeled dead chains, L_∞, then the effect of addition of photoinhibitor radicals to monomer will have a negligible effect on the measurement of the living chain MWD, $\psi(N)$, provided the distribution of S is broad. Thus, the condition $S_\infty \ll L_\infty \approx \psi_l^o$ needs to be satisfied for the effect of incorrectly labeled chains to be negligible. Now, the condition $S_\infty \ll \psi_l^o$ will be satisfied if, by the time significant addition takes place, the amount of photoinhibitor radicals (M) has dropped to a value much smaller than the total amount of living chains that are to be measured (ψ_l^o), i.e., if $M(\tau_{add}) \ll \psi_l^o$. This amounts to requiring that τ_{add} be much longer than some time scale t^*, defined such that $M(t^*) = \psi_l^o$ (see Figure 4). We calculate t^* below.

Now, in the simple case where the addition rate constant $k_{add} = 0$, photoinhibitor (M)−living chain (P) reactions actually are a small perturbation to pure M−M reactions, since the initial amount of living chains (ψ_l^o) is much smaller than the initial amount of photoinhibitor radicals.[9,10] Thus, the photoinhibitor radicals approximately obey bimolecular kinetics due to M−M reactions up to $t \approx \tau_{add}$, and hence at $t = t^*$ we have

$$\frac{M(t^*)}{M_o} = \frac{\psi_l^o}{M_o} \approx \frac{1}{1 + t^*/\tau_{kill}} \qquad (1)$$

from which $t^* \approx \tau_{kill}/r$ is immediately obtained after use of $r \equiv \psi_l^o/M_o \ll 1$. Now, using $\tau_{kill} \approx \tau^o_{living}r$, which follows from the expressions for $\tau_{kill} = 1/(k_{MP}M_o)$ and $\tau^o_{living} = 1/(k_t\psi_l^o)$, with $k_t = \mathcal{O}(k_{MP})$, we see that $t^* \approx \tau_{kill}/r \approx \tau^o_{living}$. Thus, the total amount, S_∞, of labeled dead chains produced through photoinhibitor addition to monomer will be small compared to the correctly labeled ones, $L_\infty \approx \psi_l^o$, provided $\tau_{add} \gg \tau^o_{living}$. Since $\tau^o_{living} \approx \mathcal{O}(0.1-1)$ s, this may be a rather difficult constraint to realize in practice.

Although this simple analysis is far from being rigorous or complete, it shows how sensitive the experi-

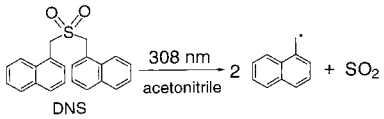

Figure 5. Photolysis of the photoinhibitor molecule dinaphthyl sulfone (DNS) yielding naphthylmethyl radicals which are relatively unreactive toward alkenes. Following coupling reaction with living chains, the naphthalene group becomes a very good fluorescent label.

ment is to photoinhibitor addition to monomer. An effect ignored above is that in the actual experiment the rate of thermal initiation, R_i, is kept constant. Since the amount of new living chains generated thermally will be of order ψ_1^o for times $t \approx \tau^o_{living}$, the effect of thermal initiation should be considered in a more detailed calculation. A more detailed analysis than the one presented here is given in ref 9, where MWDs of incorrectly labeled chains, S, are calculated.

In the following sections, we adopt various approaches to experimentally establish whether photoinhibitor radical addition to monomer is significant. We first attempt (and fail) to measure the addition rate constant, k_{add}, directly. We then present experiments performed in the absence of thermal initiator, where the only source of initiating radicals would be photoinhibitor radicals, provided self-initiation and/or impurities do not play a significant role. Finally, we test whether addition is significant by measuring the total amount of labeled dead chains ($L_\infty + S_\infty$) produced in the photocopy experiment as a function of M_o, the maximum concentration of photoinhibitor radicals produced per pulse.

B. Attempts to Measure τ_{add} by Direct Spectroscopy. We have found that the most successful photoinhibitor compounds for the photocopy experiment are arylmethyl sulfone compounds[11] such as DNS (Figure 5) and DNPMS (Figure 3). Upon photolysis, these produce, with good efficiency, two identical radicals with low reactivity toward monomer. Unfortunately, there are relatively few studies on the photochemistry and photophysics of arylmethyl sulfones as compared to carbonyl compounds.[12,13] Similarly, little quantitative information exists on the reactivity of radicals highly stabilized by aromatic structures with alkenes or alkynes,[14] another central issue for the photocopy experiment. The photochemistry of arylmethyl sulfones has been examined by Amiri and Mellor,[15] Givens and co-workers,[16] and Gould et al.[11] These and some other findings are summarized by Horspool and Armesto.[13] Photochemical and photophysical properties of naphthylmethyl radicals, on the other hand, have been studied by Amiri and Mellor,[15] Johnston and Scaiano,[17] and Gould et al.[11]

Following some preliminary success with the photoinhibitor DNS, its photophysical and photochemical properties were measured in our laboratory using a range of techniques.[10] These properties are expected to be similar in the case of DNPMS, a derivative of DNS. It has been shown by direct spectroscopy[10,15,17] that upon photolysis using 308 nm laser light, DNS cleaves to yield naphthylmethyl radicals as shown in Figure 5. How fast do these radicals add to the monomer MMA? Although no data exists in the literature on the rate constants for naphthylmethyl radical addition to alkenes, this is expected to be a "slow" process, since the radical is highly stabilized by the aromatic structure.[14,18−22] This is suggested by the work of Fischer,[14] which shows that the reactivity of radicals containing aromatic structures, such as benzyl radicals, is dominated by their stabilized electronic structures, rather than the usual steric factors. Among the few radicals stabilized with aromatic structures whose reactivity with alkenes has been studied,[14] the benzyl radical addition rate constant to methyl methacrylate (MMA) is 2100 M^{-1} s^{-1} at room-temperature.[14] It is expected that naphthylmethyl radicals produced from DNS will be much less reactive, since the naphthalene group stabilizes the radical to a much greater extent than the benzene ring in the benzyl radical. In turn, the 1-benzylnaphthyl radicals produced upon photolysis of the photoinhibitor DNPMS are expected to be even less reactive than the naphthylmethyl radical, due to their much higher steric constraints and electronic stabilization.[12,14]

The rate constant for the addition of naphthylmethyl radicals to MMA can, in principle, be measured by monitoring the naphthylmethyl radical's decay directly using the laser flash photolysis (LFP) technique, by observing the quenching of radical signals as monomer is added to the system. This well-known technique[23−25] relies on the fact that when the disappearance of the radical is dominated by reactions with monomer, the rate of disappearance of the radical will be directly proportional to the monomer concentration. Thus, a rate constant for addition can be inferred by studying the rate radicals disappear as a function of monomer concentration. In our case, however, the addition of naphthylmethyl radicals (derived from the photoinhibitor DNS, and detected through their absorption in the UV) to MMA is so slow that even when all the solvent is replaced by MMA (everything else kept constant), the rate of disappearance of the radicals is essentially unchanged for the time scales that can be probed by this technique (a few hundred microseconds). Since no quenching can be observed in these time scales, the addition time scale, $\tau_{add} \equiv 1/(k_{add}[mon])$ must be longer than the decay time in the absence of monomer, which is about 65 μs. Thus, $\tau_{add} \gtrsim 65\ \mu s$, which implies $k_{add} \lesssim 1700\ M^{-1}\ s^{-1}$, with [mon] $\cong$ 9 M for pure MMA. Comparing this to the rate constant[14] for the addition of benzyl to MMA (2100 M^{-1} s^{-1}), we see that our expectation that naphthylmethyl radicals should be less reactive than benzyl radicals was correct. However, in the photocopy experiment, the addition of photoinhibitor radicals to monomer can be neglected only if the addition occurs on a time scale τ_{add} much longer than the mean living chain lifetime, τ^o_{living} (see section II.A). Unfortunately, the upper limit put on k_{add} above is not sufficiently small to ensure that $\tau_{add} \gg \tau^o_{living}$. To illustrate this point, let us calculate τ_{add}, taking $k_{add} \cong 10\ M^{-1}\ s^{-1}$ and [mon] $\cong$ 9 M (pure MMA). We find $\tau_{add} \cong 10^{-2}$ s, shorter than $\tau^o_{living} \cong 0.1-1$ s! Finally, we note that the decay times ($\tau_{decay} = 1/(k_{MM}M_o)$) we directly measure for the photoinhibitor radicals in these LFP experiments are in fact a rough measurement of $\tau_{kill} = 1/(k_{MP}M_o)$, the time it takes to kill and label living chains in the photocopy experiment, since we expect $k_{MP} = \mathcal{O}(k_{MM})$, where k_{MM} is the coupling rate constant for two photoinhibitor radicals.

Thus, with the upper limit put on the naphthylmethyl radical reactivity using LFP, it is not possible to conclude whether addition of photoinhibitor radicals to monomer can be ignored in the photocopy method. This led us to consider alternative experimental approaches, described below.

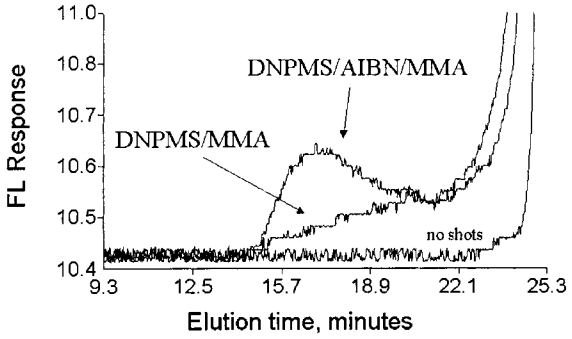

Figure 6. GPC FL chromatogram of labeled dead chains produced in the absence of thermal initiator ("DNPMS/MMA") compared with that obtained in the presence of thermal initiator ("DNPMS/AIBN/MMA"). The two samples are subjected to the same conditions: 2 min at 60, followed by 10 laser shots at relative laser intensity 2.4 (see text). No labeled polymer is observed in either case if no laser pulses are applied ("no shots"). The area under the DNPMS/MMA chromatogram (using cutoff $\mathcal{B}$ at 19 min—see Figure 8a) corresponds to a label concentration of less than 10^{-7} M.

C. Photolyses in the Absence of Thermal Initiator. To test whether photoinhibitor addition to monomer is significant, an alternative set of experiments were undertaken. In these experiments *thermal initiator is absent*, and a solution of photoinhibitor and pure monomer is subjected to the same experimental conditions as in the photocopy method for measuring living chains at steady state:[1] the samples are kept for 2−5 min at 60 °C prior to photolysis (5−10 laser shots with period $t_o \geq 10$ s).

If the photoinhibitor behaves ideally, no fluorescently labeled (or unlabeled) dead chains are expected to be observed using the FL (or RI) detector of the GPC, since no living chains are present. Any polymer produced in these experiments would result from nonideal behavior, namely from chains initiated by photoinhibitor radicals, *provided self-initiation and/or impurities do not play a role*.

In these experiments, using the photoinhibitor DNS, fluorescently labeled dead chains are indeed produced. The total amount (integrated peak areas of the FL chromatograms) of labeled chains produced from these DNS/MMA samples is very roughly 35% (depending on the cutoff chosen) of the total amount produced in the presence of thermal initiator (DNS/AIBN/MMA system). In comparison, when the photoinhibitor DNPMS is used, it is also found that some labeled polymer is produced, as seen in Figure 6. The amount of labeled polymer produced in the DNPMS/MMA system is roughly 40−50% compared to the amount produced in the presence of thermal initiator (DNPMS/AIBN/MMA).

No polymer (labeled or unlabeled) could be detected when DNPMS/MMA or DNS/MMA solutions are kept at 60 °C, but not photolyzed. For samples in which DNS is used, FL intensities from labeled polymer (using cutoff $\mathcal{B}$—see Figure 8a, section II.D, and the preceding article[1]) are about an order of magnitude higher than what is observed using DNPMS, whether in the presence or absence of thermal initiator. This indicates that DNS-derived radicals are more reactive toward monomer than DNPMS-derived ones.

Thus, at this point, addition may appear to be important for both DNS and DNPMS. However, one must ensure that the only possible source of initiating radicals in the experiments above in the absence of thermal initiator is the photoinhibitor radicals. In fact,

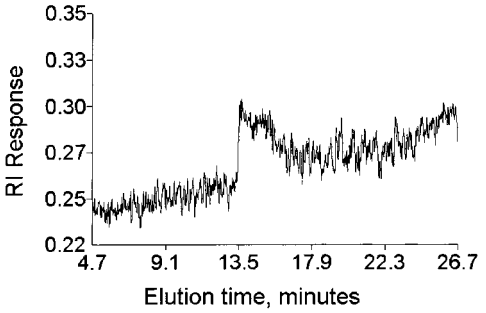

Figure 7. GPC RI chromatogram obtained from a neat MMA solution that is subjected to the same conditions as the samples in Figure 6 prior to photolysis.

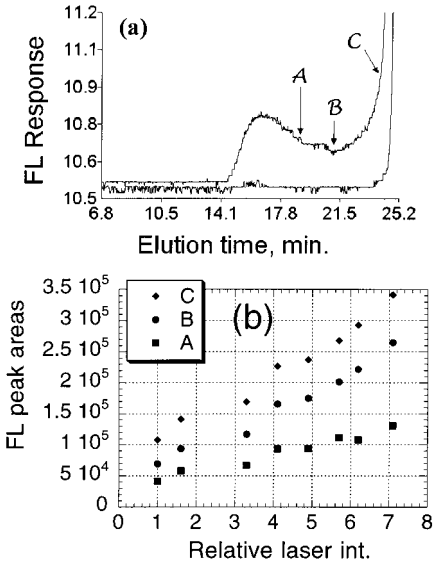

Figure 8. (a) Upper curve, typical GPC chromatogram for a DNPMS/AIBN/MMA sample, obtained using the fluorescence detector for labeled dead chains. Integration limits for the low MW (high elution times) end of the chromatograms are indicated: $\mathcal{A}$, $t \cong 19.0$ min (MW $\cong$ 27 000); $\mathcal{B}$, $t \cong 21.1$ min (MW $\cong$ 5000); $\mathcal{C}$, $t \cong 24.1$ min (MW $\cong$ 600). The chromatogram at the bottom, slightly offset vertically for clarity, is from a DNPMS/AIBN/MMA sample which is subjected only to the thermal FRP part of the experiment (no laser shots). (b) Effect of laser intensity on the integrated FL chromatograms for the DNS/AIBN/MMA system at 60 °C, using the three different cutoffs for the low MW integration limit shown in part a.

it is possible that the small amount of labeled polymer produced in the DNPMS/MMA system was due to initiation of living chains from a source *other than DNPMS-derived radicals*. To investigate this possibility, pure MMA was kept at 60 °C for 3−7 min, and analyzed by GPC, but no polymer could be detected (using the RI detector). Thus, thermal self-initiation is not a relevant source of radicals.[26,27] However, when pure MMA was photolyzed (5 laser shots, when neither initiator nor photoinhibitor was present) a small amount of very high molecular weight ($M_n^{dead} \gtrsim 1\,000\,000$) polymer was formed, barely detectable by the RI detector, as shown in Figure 7. There are no detectable signals in the FL detector in these experiments. From the integrated areas under the chromatogram peaks and using the concentration calibration of the RI detector,[1] we calculate that the amount (volume fraction) of polymer formed in these experiments is about $\phi \cong 0.02\%$, corresponding to a molar concentration of $\cong 10^{-7}$ M, using $M_n^{dead} \cong 1\,000\,000$. We note that the concentration of labeled chains produced in the experiments

using DNPMS/MMA under comparable conditions is of the same order of magnitude. This shows that the production of labeled dead chains in the DNPMS/MMA system may very well be due to living chains generated by a source *other* than the addition of photoinhibitor radicals to monomer. These propagating chains would be killed and labeled by photoinhibitor radicals when these latter are also present.

The source of radicals in experiments using pure MMA is not established. The absorption of MMA at the photolysis wavelength (308 nm) is small but measurable using a double beam scanning UV spectrophotometer (Perkin-Elmer) to be ≅0.01 in a cell with 1 cm path length (neat MMA against hexane reference). Assuming every photon absorbed by MMA results in the formation of a propagating radical, we calculate that about 10^{-7} M radicals can be formed after five pulses. It is also possible, and perhaps more plausible, that absorbance and generation of initiating radicals is due to the presence of small amounts of impurities.

Would the presence of impurities also play a role in the actual photocopy method, when thermal initiator and the photoinhibitor DNPMS are present? In the presence of thermal initiator, the sample undergoes thermal FRP for a few minutes. Any small amount of impurities (such as oxygen) which may interfere with the polymerization are expected to be consumed during this period, before the photoinhibiting laser pulses are applied. Indeed, a short induction period is always present at the beginning of the polymerization, during which time any impurities are presumably consumed by the highly reactive initiator radicals.[2,7] In the absence of thermal initiator, on the other hand, small amounts of impurities will be present at the time laser pulses are applied. Since the total amount of labeled dead polymer produced is tiny, on the order of 10^{-7} M or less when DNPMS is employed,[1] in the absence of thermal initiator impurities may significantly disturb the measurements. In the case of DNS, though, the total amount of labeled polymer is on the order of 10^{-6} M, and impurities should play a relatively smaller role.

In summary, DNPMS appears to be a better photoinhibitor than DNS, and 1-benzylnaphthyl radicals derived from DNPMS much less reactive toward monomer than are naphthylmethyl radicals derived from DNS. However, the absolute reactivity of the DNPMS-derived radicals toward monomer is difficult to assess from experiments performed in the absence of thermal initiator, due to impurities which are shown to initiate propagating chains. Such impurities are not expected to play a role in the actual photocopy experiment where the system "cleans" itself during the induction period seen during the first few minutes of the thermal polymerization. Since the experiments presented in this section are inconclusive about the role of addition of DNPMS-derived photoinhibitor radicals to monomer, we undertake another experimental approach, described below.

D. Varying the Laser Intensity: a Measure for Side Reactions. We explored the reactivity of photoinhibitor radicals toward adding to monomer by measuring the intensity of the FL chromatograms (integrated peak areas) as a function of laser intensity used in the photolysis. The FL chromatogram intensities are proportional to the total amount of labeled polymers that are in the sample ($L_\infty + S_\infty$), whether labeled intentionally (L_∞) or unintentionally (S_∞). On the other hand, the maximum concentration of photoinhibitor radicals generated per laser pulse, M_o, is proportional to the laser light intensity. If photoinhibitor radical addition to monomer is negligible (i.e., if $S_\infty \ll \psi_1^o$), we expect:

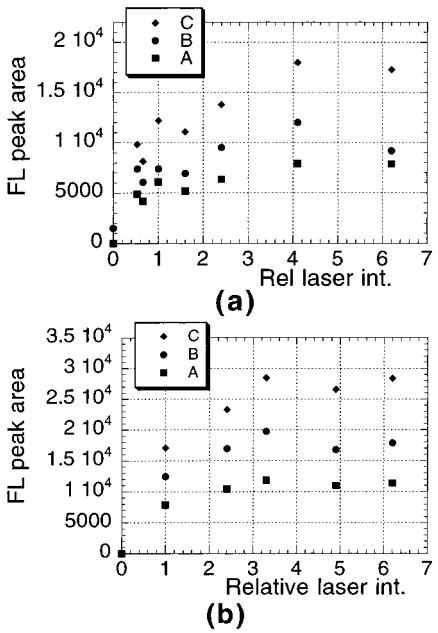

Figure 9. Effect of laser intensity on the integrated FL chromatograms for the DNPMS/AIBN/MMA system at (a) 60 and (b) 70 °C, using the three different cutoffs ($\mathcal{A}$, $\mathcal{B}$, and $\mathcal{C}$) for the low MW integration limit shown in Figure 8a.

1. At sufficiently low laser intensities the flooding condition ($r \equiv \psi_1^o/M_o \ll 1$) will not be satisfied and only a fraction of the living chains will be killed by the photoinhibitor radicals ($L_\infty \ll \psi_1^o$). The FL response should increase as the laser intensity is increased, since an increasing fraction of the living chains will be killed and labeled with increasing laser intensity (hence increasing M_o).

2. As the laser intensity is increased even further, the FL response should saturate at a certain level, when the flooding condition is satisfied and all living chains are killed and labeled by photoinhibitor radicals (i.e., $L_\infty \rightarrow \psi_1^o$).

If, however, the photoinhibitor radicals do add to monomer on a time scale τ_{add}, comparable to or faster than the mean steady-state living chain lifetime, τ^o_{living}, then the FL chromatogram intensities would increase without bound as a function of laser intensity (see section II.A), since the larger the initial concentration of photoinhibitor radicals M_o, the larger the amount of incorrectly labeled dead chains S_∞ produced. However, it is shown in ref 9 that while S_∞ is roughly proportional to M_o for smaller M_o, above a treshold value the growth becomes $S_\infty \sim \ln M_o$, i.e., the slope becomes smaller and smaller.

The FL chromatogram intensities as a function of laser intensity are plotted in Figure 8b for the DNS/AIBN/MMA system, and in Figure 9 for the DNPMS/AIBN/MMA system, using the three different cutoffs ($\mathcal{A}$, $\mathcal{B}$, and $\mathcal{C}$) for the low MW integration limit shown in Figure 8a. It can be seen that the trends are insensitive to the choice of the cutoff. The laser intensities plotted in Figures 8b and 9 are normalized for 30 mJ/pulse (relative laser intensity 1 corresponds to 30

Table 1. Quantities Measured in the Photocopy Experiment (Second Column, Using Photoinhibitor DNPMS) and Comparison with Independent Estimates or Measurements (Third Column), or Reported Values (Fourth Column), for the FRP of MMA at 60 °C, Initiated with 9×10^{-3} M AIBN ($R_i \cong 10^{-7}$ M/S)

	photocopy	indep est	lit.
$\psi^o(N)$	$\sim \begin{cases} e^{-a_1(N/\bar{N}_o)^{1-\alpha}} & (N \ll \tilde{N}) \\ e^{-a_2 N/\bar{N}_o} & (N \gg \tilde{N}) \end{cases}$ $\alpha \cong 0.2-0.5^l$ $\tilde{N}_2 = 0.59 \pm 0.04$ $N = 2-3000$		
$\bar{N}_o$	2100 ± 100	2800^a $\bar{N}_d/2 \le \bar{N}_o \le \bar{N}_d$	m
ψ_l^o (M)	$(2-3) \times 10^{-7}$	4×10^{-8} [b]	$\lesssim 10^{-7}$ [c]
ν_p (s^{-1})	5−6000		6930[d]
τ^o_{living} (s)	0.3−0.5, 2−9[e]	0.4[f]	varies
$\bar{N}_{dead}$	3300 ± 200	$\bar{N}_o \le \bar{N}_d \le 2\bar{N}_o$	varies
R_p (M/s)	$(1-2) \times 10^{-3}$ [g]	2.8×10^{-4} [h]	varies
k_t ($M^{-1}\,s^{-1}$)	$(0.8-1) \times 10^{7}$ [i]	6×10^{7} [j]	10^6-10^8 [k]
f_d	0.43		0.46[k]

[a] From $\bar{N}_o = R_p/R_i$, with calculated R_i from known rate of decomposition of AIBN and independently measured R_p. [b] From $\psi_l^o = R_p/\nu_p$, with R_p from independent measurements; ν_p from ref 31, for pure MMA. [c] Typical values. [d] From ref 31, for pure MMA. [e] Lower values from $\tau^o_{living} = \bar{N}_o/\nu_p$, with both $\bar{N}_o$ and ν_p from the photocopy experiment; higher values from curve fittings in Figure 15. [f] From $\tau^o_{living} = \bar{N}_o/\nu_p$, with $\bar{N}_o$ from footnote *a*; ν_p from ref 31, for pure MMA. [g] From $R_p = \nu_p\psi_l^o$, with both ν_p and ψ_l^o from the photocopy experiment. [h] Measured from slope of ϕ vs polymerization time data. ϕ from GPC, RI detection. [i] From $k_t = 1/(\tau^o_{living}\psi_l^o)$, with $\tau^o_{living} \cong 0.4$ s from the photocopy experiment; ψ_l^o from photocopy expt. [j] From $k_t = 1/(\tau^o_{living}\psi_l^o)$, with τ^o_{living} from footnote *f*, ψ_l^o from footnote *b*. [k] Values reported in the *Polymer Handbook*[8] for FRP of MMA at 60 °C. [l] Slightly better agreement with larger values of $\alpha_o \approx 15.5$ (9.2) for $\alpha = 0.2$ (0.5). Data for $N \ll \tilde{N}$ are also well described by $\psi^o \sim N^{-\gamma}$, with $\gamma = 0.88 \pm 0.03$. [m] We are not aware of any previous *direct* measurements of $\bar{N}_o$.

mJ/pulse). These laser intensities are measured at the exit port of the excimer laser beam, and are considerably higher than the actual light intensities falling on the sample. However, the actual light intensity falling on the sample is proportional to the values measured at the exit port.

When DNS is used as the photoinhibitor, we observe from Figure 8b that the amount of labeled polymer (proportional to FL intensity) increases nearly linearly within the range of laser intensities used. On the other hand, when DNPMS is used as the photoinhibitor, FL chromatogram intensities shown in Figure 9 appear to saturate as laser intensity is increased. These results suggest that the rate of addition of naphthylmethyl radicals (derived from DNS) to monomer is much higher than the rate of addition of 1-benzylnaphthyl radicals derived from the photoinhibitor DNPMS, and that DNPMS behaves as expected from an ideal photoinhibitor.

Let us now estimate the value of the flooding parameter, $r \equiv \psi_l^o/M_o$. We estimate $M_o \cong 10^{-6}$ M at relative laser intensity = 1, based on the known area of the laser beam falling on the sample,[1] the area of the sample facing the laser beam,[1] the quantum yield for cleavage of the photoinhibitor (taken to be 0.5 for any photoinhibitor, the value measured for DNS[10]), and the optical density of the sample at the laser wavelength of 308 nm.[1] Comparing this rough estimate for M_o with the measured concentration of living chains ($\psi_l \cong 4 \times 10^{-8}$ to 3×10^{-7} M—see the preceding article[1] and Table 1), we see that at the lowest laser intensities employed $r \lesssim 1$. That is, most of the living chains should be efficiently killed and labeled at relative laser intensities $\gtrsim 1$, and the saturation seen in Figure 9 for relative laser intensities $\gtrsim 3$ seems reasonable.

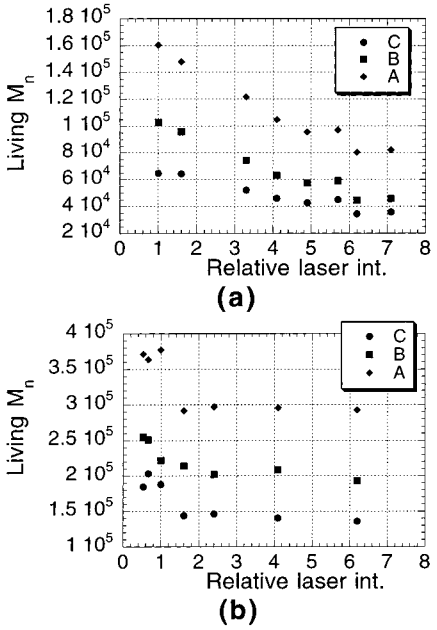

Figure 10. Effect of laser intensity on the number-average molecular weights for (a) DNS/AIBN/MMA, and (b) DNPMS/AIBN/MMA systems at 60 °C, using the three different cutoffs ($\mathcal{A}$, $\mathcal{B}$, and $\mathcal{C}$) for the low MW integration limit shown in Figure 8a.

Another quantity we have measured as a function of laser intensity is the number-average MW, M_n^{living} ($M_n^{living} = m\bar{N}$, where the molecular mass of one monomer unit is $m \cong 100$ for MMA). As in the case of living chain concentrations, this quantity should be independent of laser intensity for an ideal photoinhibitor, beyond a certain intensity. Average living chain molecular weights measured as a function of laser intensity are shown in Figure 10 for the photoinhibitors DNS and DNPMS, using different integration cutoffs. Once again, the choice the cutoff does not appear to influence the observed trends. In the case of DNS (Figure 10a), a systematic decrease in M_n^{living} is observed as a function of increasing laser intensity. In contrast, when DNPMS is used as the photoinhibitor (Figure 10b), a small decrease is seen for relative laser intensities $\lesssim 1$, but the M_n values do level off for higher laser intensities.

Thus, measurements of the laser intensity dependence of the total amount of labeled dead chains produced in the photocopy method and their mean lengths suggest, albeit indirectly, that the photoinhibitor DNPMS behaves nearly ideally.

III. Perturbing Living Chains from Steady State

In the preceding article,[1] we were concerned with experiments measuring properties of living chains in FRP at *steady state*. Although such experiments allow a number of important parameters to be measured, much more information can be obtained in experiments measuring *non-steady-state* FRPs. In this section we describe a simple non-steady-state FRP experiment, and present results from preliminary measurements. We will use the Flory−Schulz approximation (chain length independent k_t) for this section, since it remains a

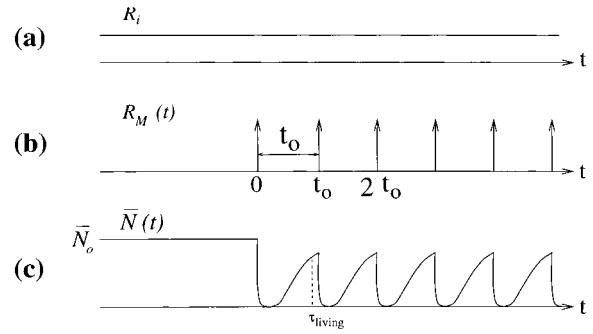

Figure 11. Timing diagram for the non-steady photocopy method. Fresh living chains are created at a constant rate R_i by the decomposition of a thermal initiator (a). Rate R_M at which photoinhibitor radicals are created is a series of δ pulses, with period t_o, which is varied in the experiment (b). Schematic sketch of the anticipated behavior for the mean living chain length, $\bar{N}$, measured in the experiment (c). For sufficiently short laser periods, living chains do not have enough time to recover their average steady state length, $\bar{N}_o$.

simple and natural framework to analyze our preliminary results.

A. How Do Living Chains Recover Following a Photoinhibitor Pulse? In experiments presented in the preceding article, the laser period between photocopying pulses, t_o, was always made much longer than the mean steady-state lifetime of living chains, τ^o_{living}; that is, $t_o \gg \tau^o_{living}$. This allowed the FRP to recover steady state, on the time scale τ^o_{living}, between each laser pulse, since the thermal initiation rate, R_i, is kept constant. Here we consider what happens as one varies the laser period, t_o, over a wide range to probe non-steady-state properties of living chains, while keeping the thermal initiation rate R_i constant (Figure 11).

As t_o is made shorter than τ^o_{living}, living chains will not find enough time to recover steady state and their mean lengths, $\bar{N}(t_o)$, will be shorter than the steady-state value, $\bar{N}_o$, as shown in Figure 11. Similarly, living chain concentrations $\psi_l(t_o)$ will be less than the concentration at steady state, ψ^o_l. In the extreme case where $t_o \ll \tau^o_{living}$, living chains will not find enough time between pulses to encounter one another and terminate before photoinhibitor radicals flood the system and kill all living chains. Thus, mean living chain lengths and concentrations will be governed by the period between photocopying laser pulses. In fact, when $t_o \ll \tau^o_{living}$, we expect that $\bar{N}$ will be linear in t_o: after a pulse, living chains will grow at rate v_p monomers per second until they are killed by photoinhibitors flooding the system with the next pulse a time t_o later. In summary, we expect (i) for laser periods shorter than a characteristic time scale $\hat{t}$ (we anticipate $\hat{t}$ to be related to τ^o_{living}), $\bar{N} \approx v_p t_o/2$, and (ii) for long laser periods ($t_o \gg \hat{t}$), $\bar{N} \approx v_p \tau^o_{living} = \bar{N}_o$. The factor $^1/_2$ in (i) above comes from the fact that there is a uniform distribution of initiation times for new living chains. At the crossover time $\hat{t}$ we have $v_p \hat{t}/2 = v_p \tau^o_{living}$, i.e., $\hat{t} = 2\tau^o_{living}$.

From the discussion above, we see that it should be possible to obtain the propagation velocity, v_p, and the mean living chain lifetime, τ^o_{living}, by measuring $\bar{N}$ as a function of t_o. Furthermore, since the photocopy experiment also measures the living chain concentration ψ_l, one can infer termination rate constants, k_t, from $\tau^o_{living} = 1/(k_t \psi^o_l)$. The last expression follows from the fact that the living chain lifetime can also be defined as the ratio of the living chain concentration ψ^o_l to the rate at which these disappear, $R_t = k_t(\psi^o_l)^2$ (using the Flory–Schulz framework).

Let us now make the above discussion more quantitative. Consider an FRP at steady state. The mixture contains photoinhibitor molecules which are inert until photocopying pulses are applied. When the first pulse is applied, all living chains are killed (and labeled) on a time scale $\tau_{kill} \ll \tau^o_{living}$, as shown in Figure 11. This first pulse is special in that it always measures the *steady state* living population, independent of the laser period t_o. Subsequent pulses, which arrive at times nt_o, where $n > 0$ is an integer, measure properties which depend on t_o. With each pulse (including the first one), all living chains are killed. Thereafter, living chains start recovering due to thermal initiation of fresh living chains, at constant rate R_i. The behavior following each pulse will be identical, provided the number of pulses is not too large, so that photoinhibitor depletion effects can be neglected. We analyze below the recovery of living chains following any one pulse. We will consider the errors introduced by the measurement of steady-state properties by the very first pulse ($n = 0$) at the end of this section. Note that the killing time scale, τ_{kill}, is unaffected by varying the laser period t_o, since it is determined by the maximum concentration, M_o, of photoinhibitor radicals created with each pulse: $\tau_{kill} = 1/k_{MP}M_o$ (see the preceding article[1]).

We assume that τ_{kill} is much shorter than the laser periods used, so that living chains are killed "instantaneously" with each pulse and that no photoinhibitor radicals survive past τ_{kill}. That is, we assume $\tau_{kill} \ll t_o^{min}$, where t_o^{min} is the shortest laser period used in the experiment. For convenience, let us label as $t = 0$ the instant the first pulse is applied. Just after this pulse the living chain concentration $\psi_l(0) = 0$, since all living chains are killed. However, a constant rate of initiation, R_i, acts on the system and generates fresh living chains. This situation is equivalent to an FRP that is suddenly turned on at $t = 0$, by a step function rate of initiation, as can readily be achieved in photoinitiated FRPs. We are interested in the evolution of the mean living chain length, $\bar{N}(t)$, as time progresses and the living chain population recovers steady state:

$$\bar{N}(t) \equiv \frac{1}{\psi_l(t)} \int_0^\infty N\psi(N, t)\, dN \qquad (2)$$

where $\psi(N, t)$ is the unnormalized molecular weight distribution (MWD) of living chains of N units at time t, and $\psi_l(t) \equiv \int_0^\infty \psi(N, t)\, dN$ is the total living chain concentration at time t. To calculate $\bar{N}(t)$, we turn to the living chain dynamics, which obey[28–30]

$$\frac{\partial \psi}{\partial t} = -v_p \frac{\partial \psi}{\partial N} - H\psi, \quad \psi(N, 0) = 0, \quad \psi(0, t) = \frac{R_i}{v_p} \qquad (3)$$

where the reaction field, namely the total termination reaction rate for a chain of length N due to all other living chains in the system, is given by

$$H(N, t) \equiv \int_0^\infty dM\, k_t(N, M, \phi)\psi(M, t) \qquad (4)$$

Let us now assume k_t to be independent of chain length, a good approximation at low conversion FRPs.[1,3,4,6] Thus, the reaction field is simply $H(t) = k_t\psi_l(t)$, from eq

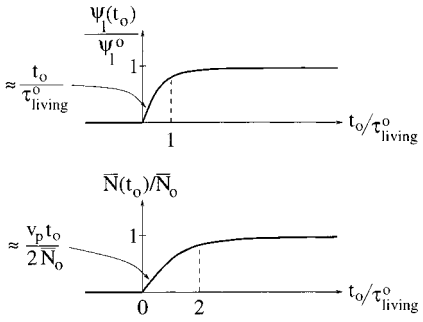

Figure 12. Theoretically predicted dependence of the scaled living chain concentration, ψ_l/ψ_l^o, and mean living chain length, $\bar{N}/\bar{N}_o$, on laser period, t_o, scaled by the mean living chain lifetime at steady state, τ^o_{living}, ignoring the effect of the first photocopying pulse. Notice that ψ_l/ψ_l^o reaches its steady-state value two times faster than $\bar{N}/\bar{N}_o$ does.

4. Multiplying eq 3 by N, and integrating over N, we obtain

$$\dot{\bar{N}}\psi_l + N(\dot{\psi}_l + k_t\psi_l^2) = v_p\psi_l \tag{5}$$

Noting that the term $\dot{\psi}_l + k_t\psi_l^2 = R_i = k_t(\psi_l^o)^2$, and using the expression for the steady-state mean living chain lifetime, $\tau^o_{living} = 1/(k_t\psi_l^o)$, we rewrite eq 5 to obtain

$$\dot{\bar{N}} + \frac{N}{\tau^o_{living}}\frac{\psi_l^o}{\psi_l(t)} = v_p \tag{6}$$

Now, $\psi_l(t)$ was calculated for an equivalent problem in ref 2:

$$\psi_l(t) = \psi_l^o \tanh\left(\frac{t}{\tau^o_{living}}\right) \tag{7}$$

Substituting the result in eq 7 into eq 6 for $\psi_l(t)$ and solving eq 6, we obtain

$$\bar{N}(t) = \bar{N}_o \tanh\left(\frac{t}{2\tau^o_{living}}\right) \tag{8}$$

Since $\bar{N}$ and ψ_l are measured at times $t = nt_o$, and the behavior is identical between any two subsequent pulses, we can replace $t \rightarrow t_o$ in eqs 7 and 8 above. Looking at the limits of interest in eq 8, we see that our expectation at the beginning of this section was correct:

$$\bar{N}(t_o) \approx \begin{cases} \dfrac{v_p t_o}{2}, & t_o \ll 2\tau^o_{living} \\ v_p\,\tau^o_{living} = \bar{N}_o, & t_o \gg 2\tau^o_{living} \end{cases} \tag{9}$$

The result for $\bar{N}(t_o)$ is schematically drawn in Figure 12 along with $\psi_l(t_o)$. It is interesting that the mean living chain length, $\bar{N}(t_o)$, recovers steady-state two times slower than the living chain concentration $\psi_l(t_o)$.

Now let us consider the effect of the first ($n = 0$) photocopying pulse which measures steady-state properties. The measurement from the first pulse will be averaged with the "true" measurements of the subsequent pulses which reflect t_o. Clearly, if a very large number of pulses are applied, the errors introduced by the first pulse measuring steady-state properties will be small. However, in practice the number of pulses are kept below 20 or 30 to avoid unwanted effects due to photoinhibitor depletion (see the preceding article). Hence, it is important to see the magnitude of the error introduced by the first pulse.

Consider first the effect on the living chain concentration in an experiment where $n + 1$ pulses are applied. The measured concentration, ψ_l^{meas}, will be an average of the effects of the first pulse which measures the steady-state concentration, ψ_l^o, and the subsequent ones which measure $\psi_l(t_o)$ (denoted ψ_l below): $\psi_l^{meas} = (\psi_l^o + n\psi_l)/(n + 1)$. Clearly, the effect of the first pulse will be most significant at the shortest laser periods t_o, where ψ_l will be small compared to ψ_l^o:

$$\psi_l^{meas} \approx \begin{cases} \psi_l, & \dfrac{\psi_l}{\psi_l^o} \gg \dfrac{1}{n} \\ \dfrac{\psi_l^o}{n+1}, & \dfrac{\psi_l}{\psi_l^o} \ll \dfrac{1}{n} \end{cases} \tag{10}$$

Now, from eq 7, for short laser periods ($t_o \ll \tau^o_{living}$) we have $\psi_l/\psi_l^o \approx t_o/\tau^o_{living}$. Using this and eq 10, we see that as the laser period t_o is made progressively shorter, the measurement will start to contain significant errors when $t_o \lesssim t_o^*$, where $t_o^* \equiv \tau^o_{living}/n$.

As for the mean living chain length, the measured value is a weighted average between $\bar{N}_o$ measured by the first pulse, and $\bar{N}(t_o)$ (denoted $\bar{N}$ below) measured by the subsequent pulses:

$$\bar{N}^{meas} = \frac{\bar{N}_o\psi_l^o + n\bar{N}\psi_l}{\psi_l^o + n\psi_l} \tag{11}$$

Now, for long laser periods ($t_o \gg 2\tau^o_{living}$) we have $\psi_l/\psi_l^o \approx 1$ and $\bar{N}/\bar{N}_o \approx 1$, from eqs 7 and 8, respectively. Thus, for these long laser periods, it follows from eq 11 that $\bar{N}^{meas} \approx \bar{N}_o$, as expected. On the other hand, when short laser periods are used ($t_o \ll \tau^o_{living}$), $\psi_l/\psi_l^o \approx t_o/\tau^o_{living}$ and $\bar{N}/\bar{N}_o \approx t_o/(2\tau^o_{living})$, from eqs 7 and 8, respectively, and eq 11 can be rewritten as (with $\delta \equiv t_o/\tau^o_{living} \ll 1$):

$$\frac{\bar{N}^{meas}}{\bar{N}} \approx \frac{(\delta_a/\delta)^2 + 1}{\delta_b/\delta + 1}, \quad \delta_a \equiv (2/n)^{1/2}, \quad \delta_b \equiv 1/n \tag{12}$$

We see from eq 12 that, for fixed n, as one lowers δ (by shortening the laser period t_o) there will be three regimes for $\bar{N}^{meas}$:

$$\bar{N}^{meas} \approx \begin{cases} \bar{N}, & \delta_a \ll \delta \\ \bar{N}(\delta_a/\delta)^2 = \bar{N}_o\delta_b/\delta, & \delta_b \ll \delta \ll \delta_a \\ \bar{N}_o, & \delta \ll \delta_b \end{cases} \tag{13}$$

Thus, in our experiments the "true" value of $\bar{N}$ will be measured only if the laser period is kept sufficiently long ($\delta_a \ll \delta$, or $t_a \ll t_o$ where $t_a \equiv \tau^o_{living}(2/n)^{1/2}$) so that we are in the first regime in eq 13. Note that the effect of the first pulse is much more severe on the measurement of $\bar{N}$ than of ψ_l.

B. Experimental Results. Laser Period Dependence of Living Chain Lengths and Concentrations. In the analysis of the previous section, it was assumed that the photocopying time, τ_{kill}, is much shorter than the minimum laser period employed in the

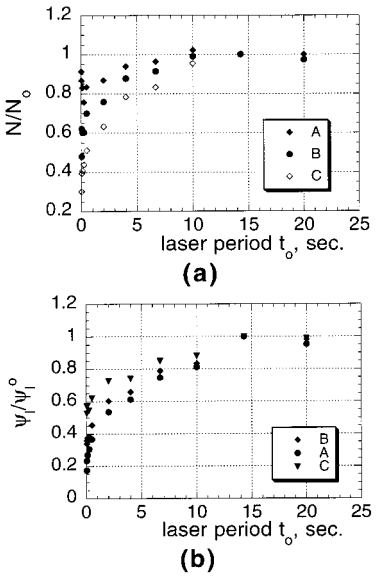

Figure 13. Experimental results for (a) $\bar{N}/\bar{N}_o$ and (b) ψ_l/ψ_l^o as a function of the laser period t_o, calculated using the three different cutoffs shown in Figure 8. Number of laser shots is $n + 1 = 20$.

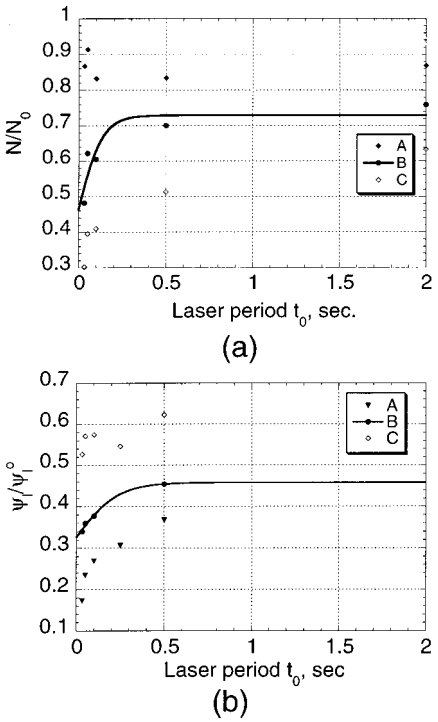

Figure 14. Same results as in Figure 13, showing shorter laser periods. (a) $\bar{N}/\bar{N}_o$ and (b) ψ_l/ψ_l^o as a function of the laser period t_o, calculated using the three different cutoffs shown in Figure 8a. Also shown are fits to a function of the form $c_1 \tanh(t_o/\tau) + c_2$ for cutoff $\mathscr{B}$: (a) $c_1 = 0.27$, $t = 0.14$ s, $c_2 = 0.46$; (b) $c_1 = 0.13$, $t = 0.23$ s, $c_2 = 0.33$.

experiment, t_o^{min}. Let us first see whether this is the case in the experiments. We estimate τ_{kill} to be $\tau_{kill} = 1/(k_{MP}M_o) \cong 1/[(10^9\ M^{-1}\ s^{-1})(10^{-6}\ M)] \cong 10^{-3}$ s, assuming the photoinhibitor radicals recombine at near diffusion-controlled rates with living chains, and using the maximum concentration of photoinhibitor radicals generated per pulse, M_o, estimated in section II.D for relative laser intensity = 1. The data presented below was actually taken using a higher relative laser intensity (=2.4); hence, M_o should be higher and τ_{kill} shorter. As for the minimum laser period, t_o^{min}, this is limited to 1/30 s by the maximum laser repetition rate available on our instrument. That is, $t_o^{min} = 0.033$ s, as compared to $\tau_{kill} \cong 10^{-3}$ s, and the ratio $\tau_{kill}/t_o^{min} \cong 0.03$ is small, as the analysis of the previous section had assumed.

Another question raised in the previous section concerns errors due to the limited number of pulses used in the system. This is a potential problem, since the very first laser pulse always measures steady-state values of $\bar{N}$ and ψ_l, while the subsequent ones measure the quantities which depend on the laser period t_o, namely $\bar{N}(t_o)$ and $\psi_l(t_o)$. In a typical experiment where 20 laser shots are applied ($n + 1 = 20$), and $\tau^o_{living} \approx 0.3$ s, we see from the analysis of the previous section that the measurements will start breaking down for laser periods $t_o \lesssim t_o^* \equiv \tau^o_{living}/n \approx 0.015$ s for $\psi_l(t_o)$ and for $t_o \lesssim t_a \equiv \tau^o_{living}(2/n)^{1/2} \approx 0.1$ s for $\bar{N}(t_o)$. Comparing these with the shortest laser periods experimentally available, $t_o^{min} \approx 0.03$ s, we see that our measurements of $\bar{N}(t_o)$ may actually contain some errors due to the effect of the first pulse. Taking $n + 1 = 20$, $\tau^o_{living} \approx 0.3$ s, and $t_o^{min} \approx 0.03$ s, we estimate, from eq 12, $\delta \cong 0.1$, $\delta_a \cong 0.3$, $\delta_b \cong 0.05$, which places us in the second regime in eq 13, with $\bar{N}^{meas} \approx \bar{N}_o\delta_b/\delta \cong 0.5\bar{N}_o$. That is, our measurements of $\bar{N}^{meas}/\bar{N}_o$ should saturate to about $^1/_2$ at the shortest laser periods employed.

In Figure 13, $\bar{N}/\bar{N}_o$ and ψ_l/ψ_l^o measured as a function of laser period, t_o, are plotted, using the three different integration cutoffs for the FL chromatograms as discussed earlier and shown in Figure 8a. Clearly, the choice of the cutoff makes significant differences in the calculated results for this experiment. It is clear from Figure 13a that using the lower cutoff $\mathscr{A}$ (corresponding to MW $\cong$ 27 000), largely misses the effect of short laser periods on $\bar{N}$. In fact, at short laser periods, many of the chains do not find enough time to grow to the cutoff size MW $\cong$ 27 000 before they are killed (and labeled) by photoinhibitor radicals. On the other hand, we see from Figure 13b that ψ_l/ψ_l^o is less sensitive to the variation of the laser period when cutoff $\mathscr{C}$ is chosen. This indicates that interference from low MW compounds may be significant using cutoff $\mathscr{C}$ (corresponding to MW $\cong$ 600). Thus, cutoff $\mathscr{B}$ appears to be the most accurate one to use, as we had argued earlier.[1]

For data obtained using cutoff $\mathscr{B}$, it can be seen in Figure 13 that there exist two distinct time scales for the evolution of both $\bar{N}/\bar{N}_o$ and ψ_l/ψ_l^o as a function of t_o. As a function of increasing t_o, first a sharp rise, in less than a second, is seen for $\bar{N}/\bar{N}_o$ and ψ_l/ψ_l^o, followed by a slower increase. The short time behavior can be distinguished more clearly in Figure 14, where the data of Figure 13 are replotted for shorter laser periods. Also shown in Figure 14 are least-squares fits to a function of the form $c_1 \tanh(t_o/\tau) + c_2$ for the data obtained using cutoff $\mathscr{B}$. From these plots, the data are not inconsistent with the predicted hyperbolic tangent dependence for both the mean living chain length and the living chain concentrations (see eqs 7 and 8), although the limited number of data points and the influence of the first pulse in these preliminary measurements prohibits a quantitative judgment about the quality of the agreement. These fits yield $\tau \cong 0.14$ s for $\bar{N}/\bar{N}_o$ (Figure 14a), and $\tau \cong 0.23$ s for ψ_l/ψ_l^o (Figure 14b). These time scales are in the right ballpark to be identified with the mean living chain lifetime, τ^o_{living}. The origin of the slower

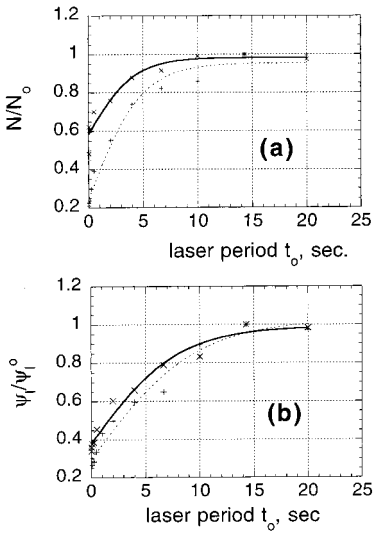

Figure 15. Data from two sets of measurements for (a) $\bar{N}/\bar{N}_o$ and (b) ψ_1/ψ_1^o as a function of the laser period t_o, calculated using cutoff $\mathscr{B}$. Fits to a function of the form $c_1 \tanh(t_o/\tau) + c_2$ are also shown: (a) $c_1 = 0.40$, $t = 4.2$, $c_2 = 0.6$ (solid line, fit to ×) and $c_1 = 0.71$, $t = 4.8$, $c_2 = 0.25$ (dashed line, fit to +); (b) $c_1 = 0.61$, $t = 7.9$ s, $c_2 = 0.38$ (solid line, fit to ×) and $c_1 = 0.73$, $t = 9.5$ s, $c_2 = 0.30$ (dashed line, fit to +).

process, which has a time constant of about 5 s (see below), however, is not clear.

Results for two different experimental runs, using cutoff $\mathscr{B}$, are plotted in Figure 15, showing fair reproducibility. The first set (crosses) is the same as the one plotted in Figure 13. For the second set (pluses) the number of shots is actually not kept constant: $n + 1 =$ 30, 20, and 10 are used for 1/30 s $\le t_o \le$ $^1/_2$ s, 1 s $\le t_o \le$ 6.67 s, and $t_o \ge 10$ s, respectively. Also plotted in Figure 15 are least-squares fits of a function, of the form $c_1 \tanh(t_o/\tau) + c_2$, to the data. From the fits for $\bar{N}/\bar{N}_o$ shown in Figure 15a, $\tau \cong 4.2-4.8$ s are obtained, while the fits for ψ_1/ψ_1^o shown in Figure 15b yield $\tau \cong 8-9$ s. These values are obviously too large to be identified with the living chain lifetime, estimated in the preceding article,[1] from the relation $\tau^o_{living} = \bar{N}_o/v_p \cong 0.3$ s, using experimentally measured[1] $\bar{N}_o \cong 2100$, and $v_p = 6930$ s^{-1} reported in ref 31.

The source of the long process is not identified. The possibility of chain transfer to monomer is excluded for the following two reasons. First, for PMMA living chains, the transfer coefficient to MMA is small[7] $C_{tr} \equiv v_{tr}/v_p \approx 10^{-5}$ where v_{tr} is the transfer velocity. That is, the characteristic time for transfer events is on the order of $\tau_{tr} = 1/v_{tr} \approx 1/(10^{-5} \times 6930/\text{s}) \approx 14$ s. Although this is not too far off the time scale for the unidentified slow process, it is incompatible with the living and dead chain lengths produced in the FRP; $\bar{N}_o \cong 2100$ and $\bar{N}_d \cong 3300$. In comparison, to see a transfer event, a chain must grow $1/C_{tr} \cong 10^5$ steps on the average. The second evidence against chain transfer is that although chain transfer would affect the mean living chain lengths, it would not effect the living chain concentrations, as the number of radicals is conserved during a transfer event. That is, if chain transfer were responsible for the slow process, this would only appear in the $\bar{N}/\bar{N}_o$ vs t_o plots and not on the ψ_1/ψ_1^o plots. A possible candidate for the slow process is interference from the SO_2 molecules released with the photolysis of the photoinhibitor molecules (Figures 3 and 5). Sulfur dioxide may indeed add reversibly to a living chain, creating a radical end group which propagates slower.[32] Although ceiling temperatures for the addition reaction are especially low for 1,1-disubstituted olefins,[32] we cannot rule out this possibility.

Recall from the previous section that for sufficiently short laser periods, living chain concentrations are expected to saturate to a value $1/(n + 1)$th their steady-state value, when a total of $n + 1$ pulses are applied (eq 10), due to the fact that the very first pulse ($n = 0$) always measures steady-state properties. From Figure 15b, where at the shortest laser periods the total number of laser shots is either 20 (crosses) or 30 (pluses), we see that the data is far from saturating to $^1/_{20}$ or $^1/_{30}$. This may be due to the limited range of laser periods explored in the experiment. Nevertheless, it is reassuring that the data points corresponding to the larger number of pulses (pluses) lies lower than the ones corresponding to the smaller number of pulses (crosses) as one moves to the shortest laser periods in Figure 15b. As for the measurement of mean living chain lengths, we expect that the effect of the first pulse should be more serious (eq 12). Indeed, the data for $\bar{N}$ (Figure 15a) does seem to be more sensitive to the number of pulses applied at the shortest laser periods than the data for ψ_1 (Figure 15b).

We saw in the previous section that for short ($t_o \ll 2\tau^o_{living}$) laser periods the mean living chain length, $\bar{N} \approx v_p t_o/2$ (eq 9), is independent of the mean living chain lifetime. This allows us to measure the propagation velocity v_p from the initial slope of the data in Figure 14. Using only the first three points in Figure 14a for cutoff $\mathscr{B}$, we obtain $v_p \cong 5000-6000$ s^{-1}, a value that is somewhat lower than the one reported in ref 31 ($v_p =$ 6930 s^{-1}). We can actually estimate living chain lifetimes $\tau^o_{living} = \bar{N}_o/v_p$, using this value of v_p and the mean living chain lengths obtained at long laser periods: $\tau^o_{living} \cong 2100/(5000/\text{s}) \cong 0.4$ s. This rather crude estimate is nevertheless the same order of magnitude as the lifetimes obtained from curve fittings above, and is in very close agreement with the estimate ($\tau^o_{living} \cong 0.3$ s) made in the preceding article[1] from measured $\bar{N}_o$, and v_p from ref 31.

We note that the measurements of $\bar{N}(t_o)/\bar{N}_o$ depend on the chain transfer rate, while the measurements of $\psi_1(t_o)/\psi_1^o$ is independent of it. Thus, in principle, measurements of both of these quantities using the photocopy method would allow one to obtain chain transfer coefficients, although the current precision of the photocopy method prohibits this, at least for MMA for which transfer coefficients are very low.[7] Nevertheless, using monomers with higher transfer coefficients one may be able to measure chain transfer rates using the photocopy method.

Overall, the preliminary data presented in this section are consistent with measurements presented in the preceding article and values reported in the literature, except for a slow process, of unidentified origin, seen in the behavior of the mean living chain lengths and living chain concentrations as a function of the laser period. Nevertheless, the non-steady-state measurements presented here represent a big step forward compared to experimental methods previously available in the field, for they allow one to follow in time directly, and with great detail, the response of living chains to controlled perturbations and complement nicely the steady-state measurements reported earlier.[1]

IV. Discussion

In this article, (i) we addressed a number of issues regarding the reactivity of the photoinhibitor radicals toward monomer and (ii) presented measurements of living chains whose steady-state is perturbed.

A potential difficulty in the photocopy method is the addition of photoinhibitor radicals to monomer. As discussed in section II.A, the experiment is quite susceptible to this type of side reaction. There, it was shown that the effect of photoinhibitor radical addition to monomer can be ignored if the addition time scale, τ_{add}, is much longer than the mean living chain lifetime, τ^{o}_{living}. Experimentally, τ_{add} is difficult to measure directly, since radical−radical recombination events provide a much faster pathway to the disappearance of photoinhibitor radicals than addition to monomer, even at very low concentrations of radicals and in neat monomer. In section II.D, we presented rather indirect experimental evidence, based on the total amount of labeled dead chains produced as a function of laser intensity—which saturates as laser intensity is increased—that addition of photoinhibitor radicals to monomer ("pollution") appears to be negligible when the compound DNPMS is employed. In comparison, theory predicts,[9] for the pure pollution case (where the only source of living chains is the pollution process), a weak, logarithmic dependence on laser intensity of the total number of labeled "pollutant" dead chains for high intensities; hence these measurements must be interpreted with some caution. In section II.C we also presented results from experiments carried out in the absence of thermal initiator, hence of living chains. In these experiments, it was found that photolysis of either DNPMS or DNS in pure MMA solutions produce some labeled dead chains. However, small amounts of polymer are also produced when only pure MMA is photolyzed, suggesting that the source of radicals (and hence of polymer) observed in experiments where only photoinhibitor dissolved in monomer is photolyzed is not necessarily the photoinhibitor molecules. We thus argued that the source of initiating radicals could be impurities and that one should be very careful before extrapolating the results obtained in the photoinhibitor−monomer system to the actual photocopy experiment. The actual photocopy experiment is less prone to impurities, since these would be "chewed up" during the thermal polymerization part of the experiment. In summary, the issue of photoinhibitor radical addition to monomer has not yet been completely resolved, though our indirect results suggest DNPMS-derived radicals behave nearly ideally.

In the second part of this article, we presented our first measurements of living chains perturbed from the steady state. At $t = 0$, all living chains are suddenly removed from the FRP system using a photocopying laser pulse, that is a "vacuum" is created. However, the rate of thermal initiation of new living chains, R_i, is unchanged; thus, living chains start recovering their steady-state concentrations and lengths following the pulse. In analogy with "post-effect"[33−37] experiments where R_i is turned off at $t = 0$ and the response of the FRP is monitored thereafter, the non-steady-state experiments presented here may be termed "reverse post-effect": the recovery from vacuum (as compared to the decay from steady state) is measured. In our reverse post-effect measurements, the dependence of the mean living chain length, $\bar{N}$, and the living chain concentration, ψ_l, on the period of the photoinhibiting laser shots allows propagation velocities, v_p, and mean steady state living chain lifetimes τ^{o}_{living} to be measured. Coupling these with steady state information obtained using sufficiently long laser periods (as explained in detail in the preceding article[1]), termination rate constants ($k_t = 1/(\tau^{o}_{living}\psi^{o}_{l})$), and rates of polymerization ($R_p = v_p\psi^{o}_{l}$), are readily obtained. In the photocopy method the dead population is measured simultaneously with the living one. Comparison of the mean dead chain length, $\bar{N}_d$, with the mean living chain length, $\bar{N}$, allows the fraction of living chains terminating via disproportionation, f_d, to be extracted. Previously, it was difficult to conceive that one could obtain all these quantities in a single set of experiments. Results for the FRP of MMA at 60 °C from the photocopy method are summarized in the second column of Table 1. These are compared with independent estimates or measurements shown in the third column and with values reported in the literature in the fourth column. This is the same table presented in the preceding article,[1] complemented here with information obtained from non-steady-state experiments. As can be seen from the entries in the third column of Table 1, calculations of relevant quantities using the known rate of initiation, R_i, independent measurement of the polymerization rate, R_p, and reliable propagation velocities, v_p, from the literature are, in general, consistent with the quantities measured directly in the photocopy experiment. Values available in the literature (fourth column) are also in fair agreement with the values obtained in the photocopy experiment.

An unexpected result is that two distinct time scales are observed in the reverse post-effect experiments for the recovery of ψ_l and $\bar{N}$. The shorter time scale, of about 0.1−0.3 s, is identified with the mean living chain lifetime, τ^{o}_{living}, while a longer time scale, of about 5 s, is also present. The origin of this slower process has not yet been clarified, though interference from SO_2 released upon photolysis of photoinhibitor molecules is a possibility.

In the non-steady-state measurements presented in section III.B, it was shown that there is a limitation due to the fact that the first pulse in these experiments always measures steady-state properties. This effect becomes increasingly severe as one moves to shorter laser periods. Similarly, a limit was put on the shortest laser periods to be used ($t_o^{min} \gg \tau_{kill}$) in order to simplify the analysis. A third and more severe limitation of the method in its current version is due to thermal initiation persisting during the photocopying process. Thus, some post-laser-flash initiated living chains react with surviving photoinhibitor radicals, creating labeled dead chains which distort the measured living chain MWDs. All of these limitations can be eliminated completely if, instead of thermal initiation photochemical initiation is used as depicted in Figure 16: continuous photolysis of the initiator is started at $t = 0$ and is stopped at $t = t_{on}$ (Figure 16a), just before a photoinhibiting pulse is applied (Figure 16b). Of course, in such an experiment one must choose a photoinitiator which absorbs at a different wavelength than the photoinhibitor does.

Actually, using photoinitiation opens the way to an unlimited number of different ways to modulate the rate of initiation, $R_i(t)$. A very simple variation of the experiment just described involves adding a delay between the time initiation is turned off and the time

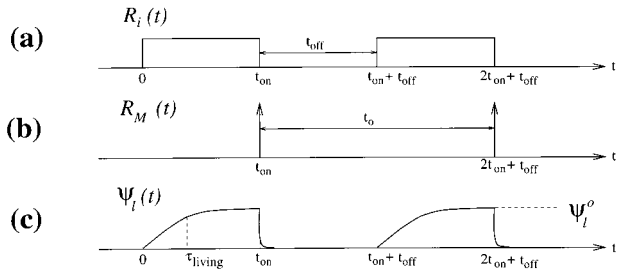

Figure 16. Timing diagram for the proposed photocopy experiment using photochemical initiation. (a) The rate of initiation is a rectangular wave in time, with light period t_{on} and dark period t_{off}. Such a modualtion can easliy be generated using a rotating sector[2] between the light source and the sample. (b) The rate photoinhibitor radicals are generated via a laser is a series of δ-pulses with period t_o. These pulses arrive at the end of the light periods of initiation. (c) Schematic of the anticipated behavior for the total living chain concentration: ψ_l increases from zero to its steady-state value (ψ_l^o) during the light periods. As soos as a light period ends, all living chains are killed and labeled by photoinhibitor radicals.

the photoinhibiting pulse arrives. Monitoring the decay of the amount of labeled chains for increasing delay times is expected to reflect the living chain lifetime, τ^o_{living}. This would be a post-effect type of experiment, except that the whole MWD would be monitored rather than just $\psi_l(t)$ as is typically done. It is also conceivable to use a second laser of a different color to initiate polymerization, rather than a continuous source of light. Actually, an experiment of this spirit has already been carried out by Holdcroft and Guillet,[19] who used the photoinhibitor 2-naphthalenemethyl-1-naphthyl acetate (NMNA) and initiator AIBN. They initiated the polymerization using 367 nm laser light (where AIBN absorbs) and stopped it using 308 nm laser pulses where NMNA absorbs, but unfortunately, they found that NMNA interfered with the polymerization.

So far the photocopy experiment has been applied only to low conversion FRPs, which are relatively well understood, to test the feasibility of the method and validate it. Actually, the long-term goal is to study *high conversion* FRPs, about which much less is known experimentally and first principles theoretical predictions were lacking until recently.[28,29,38,39] A particularly fascinating, little understood, and technologically very important phenomenon observed at high conversions ($\phi \gtrsim 10\%$ for MMA) is the "Trommsdorff", or the "gel effect", where the rates of polymerization autoaccelerate.

There are no obvious fundamental limitations for the application of the photocopy method to high conversion FRPs. The presence of large amounts of polymer (e.g., a $\phi \cong 20-30\%$ solution of PMMA dissolved in MMA) is expected to have only a minor effect (of order unity) on the photocopying time scale, $\tau_{kill} = 1/(k_{MP}M_o)$. This is because it is well established that small molecule diffusion (which would influence the rate constant $k_{MP}M_o$) is affected only to a minor degree in moderately dilute polymer solutions due to the presence of polymer.[40,41] We note that a decrease in the rate constant k_{MP} can be compensated for by increasing the laser intensity (hence the maximum photoinhibitor radical concentration M_o), keeping τ_{kill} sufficiently short. This is unlike, e.g., the rotating sector method[2] where dilatometric measurements become difficult to perform at high conversions.

Acknowledgment. We thank Dimitris Vavylonis (Greek Army), Oleg Bychuk and Igor Zavarine for valuable discussions, and to Steffen Jockusch for his help with laser equipment. We also thank an anonymous referee for drawing our attention to possible interference from SO_2. This work was supported by the National Science Foundation under grant no. CHE-97-07495. E.K. gratefully acknowledges support by an Institut Curie post-doctoral fellowship.

References and Notes

(1) Karatekin, E.; Landis, M.; Lem, G.; O'Shaughnessy, B.; Turro, N. J. *Macromolecules* **2001**, *34*, 8187.
(2) Flory, P. *Principles of Polymer Chemistry*; Cornell University Press: Ithaca, NY, 1971.
(3) Friedman, B.; O'Shaughnessy, B. *Macromolecules* **1993**, *26*, 5726−5739.
(4) Friedman, B.; O'Shaughnessy, B. *Europhys. Lett.* **1993**, *23*, 667−672.
(5) O'Shaughnessy, B. *Phys. Rev. Lett.* **1993**, *71*, 3331; *Macromolecules* **1994**, *27*, 3875.
(6) Friedman, B.; O'Shaughnessy, B. *Int. J. Mod. Phys. B* **1994**, *8*, 2555−2591.
(7) Odian, G. *Principles of Polymerization*; John Wiley and Sons: New York, 1981.
(8) Brandrup, J.; Immergut, E. H.; Grulke, E. A.; Abe, A.; Bloch, D. R. *Polymer Handbook*, 4th ed.; Wiley: New York, 1999.
(9) Karatekin, E.; O'Shaughnessy, B.; Turro, N. J. **2001**, Theory of Photocopying Living Chain Distributions. 2001, in preparation.
(10) Karatekin, E. Dynamics of Free Radical Polymerization. Ph.D. Thesis, Columbia University, New York, 1999.
(11) Gould, I. R.; Tung, C. H.; Turro, N. J.; Givens, R. S.; Matuszewski, B. *J. Am. Chem. Soc.* **1984**, *106*, 1789−1793.
(12) Turro, N. J. *Modern Molecular Photochemistry*; University Science Books: Mill Valley, CA, 1991.
(13) Horspool, W.; Armesto, D. *Organic Photochemistry: A Comprehensive Treatment*; Ellis Horwood PTR Prentice Hall: New York, 1992.
(14) Fischer, H. In *Factors Controlling the Addition of Carbon Centered Radicals to Alkenes and Alkynes;* Minisci, F., Ed.; NATO ASI Series. Partnership sub-series 3, High technology Kluwer: Dordrecht, The Netherlands, 1997; Vol. 27, pp 63−78.
(15) Amiri, A.; Mellor, J. M. *J. Photochem.* **1978**, *9*, 571−575.
(16) Givens, R. S.; Hrinczenko, B.; Liu, J. H. S.; Matuszewski, B.; Tholencollison, J. *J. Am. Chem. Soc.* **1984**, *106*, 6, −1779−1789.
(17) Johnston, L. J.; Scaiano, J. C. *J. Am. Chem. Soc.* **1985**, *107*, 6368−6372.
(18) Holdcroft, S.; Yuen, K. H.; Guillet, J. E. *J. Polym. Sci.: Part A: Polym. Chem.* **1990**, *28*, 1495−1505.
(19) Holdcroft, S.; Guillet, J. E. *J. Polym. Sci.: Part A: Polym. Chem.* **1991**, *29*, 729−737.
(20) Holdcroft, S.; Tang, B.-Z.; Guillet, J. E. *J. Chem. Soc., Chem. Commun.* **1991**, pages 280−282.
(21) Holdcroft, S.; Guillet, J. E. *Macromolecules* **1991**, *24*, 1210−1212.
(22) Modi, P. J.; Guillet, J. E.; Scaiano, J. C.; Wintgens, V. *J. Photochem. Photobiol. A: Chem.* **1994**, *81*, 87−91.
(23) Jockusch, S.; Turro, N. J. *J. Am. Chem. Soc.* **1998**, *120*, 11773−11777.
(24) Jockusch, S.; Turro, N. J. *J. Am. Chem. Soc.* **1999**, *121*, 3921−3925.
(25) Martschke, R.; Farley, R. D.; Fischer, H. *Helv. Chim. Acta* **1997**, *80*, 1363−1374.
(26) Stickler, M.; Meyerhoff, G. *Polymer* **1981**, *22*, 928−933.
(27) Lingnau, J.; Stickler, M.; Meyerhoff, G. *Eur. Polym. J.* **1980**, *16*, 785−791.
(28) O'Shaughnessy, B.; Yu, J. *Macromolecules* **1994**, *27*, 5067−5078.
(29) O'Shaughnessy, B.; Yu, J. *Macromolecules* **1994**, *27*, 5079−5085.
(30) O'Shaughnessy, B.; Yu, J. *Phys. Rev. Lett.* **1994**, *73*, 1723−1726.
(31) Hutchinson, R. A.; Aronson, M. T.; Richards, J. R. *Macromolecules* **1993**, *26*, 6410−6415.
(32) Florjańczyk, Z.; Raducha, D. *Polish, J. Chem.* **1995**, *69*, 481−508.

(33) Yamada, B.; Kageoka, M.; Otsu, T. *Macromolecules* **1991**, *24*, 5234−5236.
(34) Zhu, S.; Tian, Y.; Hamielec, A. E.; Eaton, D. R. *Macromolecules* **1990**, *23*, 1144−1150.
(35) Shen, J.; Tian, Y.; Wang, G.; Yang, M. *Makromol. Chem.* **1991**, *192*, 2669−2685.
(36) Shen, J.; Wang, G.-B.; Yang, M.-L.; Zheng, Y.-G. *Polym. Int.* **1992**, *28*, 75−79.
(37) Kamachi, M.; Kohno, M.; Kuwae, Y.; Nozakura, S.-I. *Polym. J.* **1982**, *14*, 749−752.
(38) O'Shaughnessy, B.; Yu, J. *Macromolecules* **1998**, *31*, 5240−5254.
(39) O'Shaughnessy, B.; Yu, J. *Phys. Rev. Lett.* **1998**, *80*, 2957−2960.
(40) de Gennes, P. G. *Scaling Concepts in Polymer Physics*; Cornell University Press: Ithaca, NY, 1985.
(41) Doi, M.; Edwards, S. F. *The Theory of Polymer Dynamics*; Clarendon Press: Oxford, England, 1986.

MA0100798